

# MicroRNA-296, a suppressor non-coding RNA, downregulates *SGLT2* expression in lung cancer

XIAOTIAN ZHANG<sup>1\*</sup>, XINJU ZHANG<sup>2\*</sup>, XIAOMIN LIU<sup>2</sup>, PENGFEI QI<sup>2</sup>,  
HUI MIN WANG<sup>2</sup>, ZHONGLIANG MA<sup>2</sup> and YIMIN CHAI<sup>1</sup>

<sup>1</sup>Department of Orthopedic Surgery, Shanghai Jiao Tong University Affiliated Sixth People's Hospital, Shanghai 200233;  
<sup>2</sup>Laboratory for Noncoding RNA and Cancer, School of Life Sciences, Shanghai University, Shanghai 200444, P.R. China

Received May 9, 2018; Accepted August 28, 2018

DOI: 10.3892/ijo.2018.4599

**Abstract.** Non-small cell lung cancer (NSCLC) is one of the most common types of cancer worldwide and has the highest mortality rate in China. MicroRNAs (miRNAs or miRs) are involved in tumorigenesis and their important role in cancer is becoming increasingly apparent. The expression of miR-296-5p in particular has been shown to be significantly downregulated in lung cancer. Sodium-glucose co-transporter-2 [*SGLT2*, also known as solute carrier family 5 member 2 (*SLC5A2*)] is an oncogene that promotes tumorigenesis. In this study, we aimed to determine the role of miR-296-5p in lung cancer and whether this involves the targeting of *SGLT2*. For this purpose, we examined miR-296-5p and *SGLT2* expression in human lung cancer samples and cell lines by RT-qPCR and western blot analysis. In addition, the data analysis website TCGA was used for survival analysis with respect to *SGLT2* expression. The effects of miR-296-5p were also examined on cell proliferation and cell cycle progression using respective assays. The results demonstrate that miR-296-5p is significantly downregulated in NSCLC tissues. Additionally, it is demonstrated that *SGLT2* is directly targeted by miR-296-5p. Furthermore, our data reveal that the knockdown of *SGLT2* using siRNA inhibits cell proliferation and impedes cell cycle progression. Collectively, data suggest that miR-296-5p not only inhibits NSCLC by downregulating *SGLT2* expression, but also acts

as a novel regulator of aberrant lung cancer cells to limit lung cancer progression.

## Introduction

Lung cancer is the leading cause of cancer-related mortality worldwide, with non-small cell lung cancer (NSCLC) accounting for almost 80% of all lung cancer cases (1,2). In China, the overall 5-year survival rate for NSCLC patients is approximately 15% and the rate of recurrence remains high (3-7). Despite advances in early detection and diagnosis, chemical and immunotherapy, precision radiotherapy, and expert surgical intervention, eradicating cancer in patients remains a major challenge. Although our understanding of cancer cell biology has made significant progress, a definite cure for most types of cancer does not exist at present (8-11). Therefore, there is urgent need to discover novel biomarkers for diagnosis and treatment.

MicroRNAs (miRNAs or miRs) are small non-coding single-stranded RNAs of approximately 20-23 nt in length that regulate gene expression by binding to the 3'-untranslated regions (3'-UTR) of mRNAs (12-14). The expression levels of miRNAs have profound effects on cancer progression and human carcinogenesis (15). The expression of miR-296-5p has been shown to be significantly downregulated in lung cancer (3,16,17), breast cancer (18), diabetes (19-21) and other types of cancer and diseases (17,22,23). Therefore, exploring the function of miR-296-5p and the role of its possible target genes is essential to the understanding of the molecular mechanism of this miRNA in NSCLC. Sodium-glucose co-transporter-2 [*SGLT2*, also known as solute carrier family 5 member 2 (*SLC5A2*)], a sodium-dependent glucose transporter, is a common therapeutic target in the treatment of diabetes (24). In addition, *SGLT2* promotes the development of pancreatic and prostate adenocarcinomas (25) and increases lung cancer metastasis (26). Therefore, we hypothesized that miR-296-5p may play a pivotal role in lung cancer tumorigenesis by targeting *SGLT2*.

In this study, we aimed to investigate this hypothesis. We demonstrate that miR-296-5p is downregulated in NSCLC patient samples and NSCLC cell lines. Moreover, we demonstrate that miR-296-5p directly targets *SGLT2*. These results may provide a potential molecular therapeutic target for the occurrence and development of NSCLC.

**Correspondence to:** Dr Zhongliang Ma, Laboratory for Noncoding RNA and Cancer, School of Life Sciences, Shanghai University, 381 Nanchen Road, Shanghai 200444, P.R. China  
E-mail: zlma@shu.edu.cn

Dr Yimin Chai, Department of Orthopedic Surgery, Shanghai Sixth People's Hospital, Jiao Tong University, 600 Yishan Road, Shanghai 200233, P.R. China  
E-mail: ymchai@sjtu.edu.cn

\*Contributed equally

**Key words:** non-small cell lung cancer, proliferation, cell cycle, miR-296-5p, sodium-glucose co-transporter-2

## Materials and methods

**Tissue samples.** All NSCLC samples and non-tumor samples (also termed paracancerous tissue, i.e., tissue adjacent to cancerous tissue) were obtained from the Department of Oncology, Shanghai Chest Hospital (Shanghai, China) from October, 2014 to August, 2016 and their use was approved by the Ethics Committee of Shanghai Hospital and consent was obtained from all the patients. All the details of the tissue samples used in this study are listed in Table I. We obtained the corresponding results by analyzing the specific information of the patient tissue samples, such as sex, stage and size. Tumor size is the primary determinant of prognosis and metastasis. A previous study demonstrated that a small tumor size ( $\leq 3$  cm) is associated with a lower probability of metastasis (27). Moreover, in a previous study, we demonstrated that miR-18a-targeted interferon regulatory factor 2 (IRF2) expression was downregulated in tumor tissues, and likely related to tumor size (28). Thus, in this study, we also used this method to assay the function of miR-296 in lung cancer.

**Cell culture and cell transfection.** The BEAS-2B, 16HBE and 293T cells were obtained from the Cell Bank, China Academy of Sciences (Shanghai, China). The A549, H1975, PC-9 and H1299 cells were purchased from the American Type Culture Collection (ATCC, Manassas, VA, USA). The A549, BEAS-2B, 293T and PC-9 cells were cultured in DMEM (Gibco). The H1975 and H1299 cells were cultured in RPMI-1640 medium. The culture conditions were set at 37°C in a 5% CO<sub>2</sub> humidified environment. NSCLC cells were cultivated in 90% medium, 10% fetal bovine serum (FBS, HyClone Laboratories, Logan, UT, USA), 100 µg/ml penicillin, 100 µg/ml streptomycin (Gibco) and antibiotic cocktail. The BEAS-2B cell line was originally isolated from the normal bronchial epithelium.

The A549 and H1299 cells were transiently transfected with 30 nM miR-296-5p mimic, a negative control mimic (NC) and 100 nM SGLT2 siRNA (3 siSGLT2), or negative control siRNA (siNC) (Guangzhou RiboBio Co., Ltd., Guangzhou, China) using Invitrogen™ Lipofectamine 2000 (Thermo Fisher Scientific, Waltham, MA, USA) kit according to the manufacturer's instructions. The sequences of the mimics and the siRNAs are presented in Table II. It is worth noting that we selected siSGLT2-3, the most effective from the 3 siRNAs against SGLT2, for use in the follow-up experiments. At 24 to 48 h post-transfection, the cells were used for RT-qPCR, cell proliferation analysis, colony formation analysis, cell cycle analysis and western blot analysis.

**RNA isolation, reverse transcription and RT-qPCR analysis.** Total RNA was extracted from the cells and the patient tissues using TRIzol reagent (Sangon Biotech, Shanghai, China). The PrimeScript™ 1st Strand cDNA Synthesis kit (Takara, Dalian, China) was used for reverse transcription. At the same time, the PrimeScript® miRNA First-Strand cDNA Synthesis SuperMixQuantMir cDNA kit (Transgen Biotech, Beijing, China) was used to synthesize a cDNA library of miRNAs. mRNA and miRNA expression levels were quantified by RT-qPCR using SYBR-GreenII (Takara) and a CFX96™ Real-time System (Bio-Rad, Hercules, CA, USA). The annealing temperature of the SGLT2 mRNA was 53°C, for the duration of 1 min at 72°C,

for 37 cycles, while the annealing temperature of miR-296 was 56°C, for the duration of 1 min at 72°C, for 39 cycles. The data for relative quantification of mRNAs and miRNAs were normalized to 18S RNA and U6 snRNA, respectively. The expression was determined using the relative quantification ( $2^{-\Delta\Delta C_q}$ ) method (29). The primer sequences are presented in Table III.

**Cell proliferation assay.** The cell proliferation assay was performed as previously described (30). The NSCLC cells were plated on a 96-well microplate. The density was  $2 \times 10^3$  or  $4 \times 10^3$  cells per well and the cells were incubated at 37°C in 5% CO<sub>2</sub>. After 24, 48 and 72 h of culture, 8 µl of CCK-8 (Dojindo, Tokyo, Japan) were added. The cultures were then returned to the incubation conditions (37°C in 5% CO<sub>2</sub>) for 2 h. The light absorbance at 450 nm was measured daily with a microplate reader, FLx8 (BioTek, Winooski, VT, USA). Each point was measured from 3 replicate wells.

**Colony formation assay.** The colony formation assay was performed as previously described (31). At 37°C in a 5% CO<sub>2</sub> humidified environment, the cells were plated in 6-well plates at 300 or 600 cells per well and incubated for 2 weeks. Colonies were stained with crystal violet (Haoranbio, Shanghai, China) (0.5% w/v) for 12 min at room temperature following fixation with methanol, and then counted. Experiments were performed in triplicate.

**Cell cycle analysis.** Cell cycle analysis was performed as previously described (32). The cells ( $10^6$ /ml) were seeded in 6-well plates and transfected after 24–48 h in culture. The cells were then subjected to propidium iodide (PI) (BD Pharmingen, San Diego, CA, USA) staining at 4°C for 15 min. The results were determined with a MoFlo XDP flow cytometer (Beckman Coulter, Inc., Brea, CA, USA). FlowJo software (Tree Star Inc., Brea, CA, USA) was used for data analysis. The experiments were performed in triplicate.

**Dual luciferase reporter assay.** The dual luciferase reporter assay was performed as previously described (33). The 3'-UTR of the target gene (SGLT2) was amplified and inserted downstream of the Firefly luciferase reporter gene in the pGL3 miReport vector (Promega, Madison, WI, USA), named pGL3-SGLT2-3'-UTR. Mutated SGLT2 sequences were also constructed (pGL3-SGLT2-3'-mUTR), and confirmed by sequencing (Sangon Biotech). Moreover, the QuikChange Mutagenesis kit was used to conduct site-directed mutagenesis of the 3'-UTR. To measure luciferase activity, the 293T cells were cultured in 24-well plates. At 60–80% confluence, the 293T cells were co-transfected with 400 ng of luciferase vector pGL3-SGLT2-3'-UTR or pGL3-SGLT2-3'-mUTR and miR-296-5p mimic or NC miRNA. We also used 100 nM with 20 ng plasmid expressing the Renilla luciferase gene (pRL, Promega) as a final concentration for transfection efficiency as a control. Following incubation for 48 h, the luciferase activity was determined by an Orion II Microplate Illuminometer (Titertek-Berthold, South San Francisco, CA, USA). The primer sequences are presented in Table III.

**Western blot analysis.** Western blot analysis was performed as previously described (28). Total protein from the A549 and

Table I. The clinicopathological characteristics of the 46 patients with non-small cell lung cancer.

No.	Sex	Age	Specimen type	Histological type	Lymphatic invasion	TNM
1	M	47	Pneumonectomy	Adenocarcinoma		T1bN0M0
2	M	78	Lobectomy	Adenocarcinoma		T2aN0M0
3	F	67	Pneumonectomy	Adenocarcinoma		T2N1M0
4	M	54	Lobectomy	Adenocarcinoma		T4N0M0
5	M	67	Lobectomy	Adenocarcinoma	Absent	T2aN0M0
6	F	53	Lobectomy	Squamous cell carcinoma	Absent	T3N0M0
7	M	67	Lobectomy	Adenocarcinoma		T2aN0M0
8	F	62	Lobectomy	Adenocarcinoma	Absent	T2aN0M0
9	F	75	Lobectomy	Adenocarcinoma	Absent	T2aN0M0
10	F	58	Lobectomy	Adenocarcinoma		T2aN1M0
11	F	65	Lobectomy	Adenocarcinoma	Present	T2aN0M0
12	M	72	Lobectomy	Adenocarcinoma		T2aN0M0
13	M	64	Lobectomy	Adenocarcinoma	Absent	T1aN0M0
14	F	62	Lobectomy	Adenocarcinoma	Present	T2aN0M0
15	M	65	Lobectomy	Adenocarcinoma		T4N2M0
16	M	58	Lobectomy	Squamous cell carcinoma	Present	T3N2M0
17	M	50	Lobectomy	Adenocarcinoma		T2aN0M0
18	M	60	Lobectomy	Adenocarcinoma	Absent	T1bN0M0
19	M	67	Lobectomy	Adenocarcinoma	Absent	T2aN0M0
20	M	71	Lobectomy	Adenocarcinoma	Present	T1bN0M0
21	F	64	Lobectomy	Adenocarcinoma	Absent	T2aN0M0
22	M	62	Lobectomy	Adenocarcinoma	Absent	T2aN0M0
23	M	58	Lobectomy	Adenocarcinoma	Present	T2aN0M0
24	M	70	Lobectomy	Adenocarcinoma	Present	T3N0M0
25	M	59	Lobectomy	Adenocarcinoma	Present	T2aN0M1a
26	F	72	Lobectomy	Adenocarcinoma	Absent	T2aN0M0
27	M	51	Lobectomy	Adenocarcinoma	Absent	T1bN0M0
28	M	51	Lobectomy	Adenocarcinoma	Absent	T1aN0M0
29	F	55	Lobectomy	Adenocarcinoma	Absent	T1bN0M0
30	F	53	Lobectomy	Squamous cell carcinoma		T3N0M0
31	M	54	Lobectomy	Squamous cell carcinoma		T4N2M0
32	M	67	Lobectomy	Adenocarcinoma	Absent	T2aN0M0
33	M	49	Lobectomy	Adenocarcinoma	Present	T2bN2M0
34	M	65	Lobectomy	Squamous cell carcinoma	Absent	T1bN0M0
35	M	65	Lobectomy	Squamous cell carcinoma		T2aN2M0
36	M	67	Lobectomy	Squamous cell carcinoma	Absent	T2aN1M0
37	M	51	Lobectomy	Adenocarcinoma	Absent	T1bN0M0
38	F	71	Lobectomy	Adenocarcinoma	Absent	T3N0M0
39	F	58	Lobectomy	Adenocarcinoma	Present	T2aN1M0
40	F	67	Lobectomy	Adenocarcinoma	Present	T2N1M0
41	M	68	Lobectomy	Adenocarcinoma	Absent	T3N0M0
42	M	70	Lobectomy	Adenocarcinoma	Absent	T3N0M0
43	M	71	Lobectomy	Adenocarcinoma	Absent	T1bN0M0
44	M	67	Lobectomy	Squamous cell carcinoma	Present	T2aN1M0
45	F	77	Lobectomy	Adenocarcinoma	Present	T4N3M0
46	F	55	Lobectomy	Adenocarcinoma	Absent	T1bN0M0

H1299 cells was extracted using RIPA lysis buffer (CWBIO, Beijing, China) and a Protein BCA Assay kit (Bio-Rad) was used to quantify the protein content. Protein samples were separated

by 10% SDS-PAGE and transferred to polyvinylidene difluoride (PVDF) membranes (Millipore Corporation, Billerica, MA, USA). After blocking in 5% powdered milk for at least 1 h at

Table II. The sequences of the mimic and siRNAs used in this study.

Mimic/siRNA	Sequence
NC mimic	UUUGUACUACACAAAAGUACUG
miR-296-5p mimic	AGGGCCCCCCCUCUAAUCCUGU
siNC	TTCTCCGAACGTGTACACGT
siSGLT2-1	CGGGTCTCTTCGACAAATA
siSGLT2-2	GGCCCTGATTGACAATCCT
siSGLT2-3	CCTGCATCCTCATGGGTTA

room temperature, the membranes were incubated with rabbit anti-SGLT2 (ab37296; Abcam, Cambridge, MA, USA), and anti- $\beta$ -actin antibodies (CST 4970L; Cell Signaling Technology, Danvers, MA, USA) at 1:1,000 overnight at 4°C. The membranes were washed and incubated with a horseradish peroxidase (HRP)-conjugated secondary antibody (1:10,000; CST 7074S; Cell Signaling Technology) for 1 h at room temperature. Subsequent visualization was detected using a chemiluminescent HRP substrate (Millipore Corporation) and imaging with an E-Gel Imager. Densitometry (ImageJ software, 1.51d 16; June, 2016) was used to quantify the relative protein expression of SGLT2, following normalization to  $\beta$ -actin.

**Statistical analysis.** The results are expressed as the group means  $\pm$  SEM and analyzed using GraphPad Prism 5 software (GraphPad Software, Inc., La Jolla, CA, USA), using t-tests for two-group comparisons. The expression of miR-296-5p in the different cell lines was determined by one-way ANOVA followed by Tukey's Honest Significant difference post-hoc test. Moreover, miRNA target prediction databases were used, including TargetScan ([http://www.targetscan.org/vert\\_71/](http://www.targetscan.org/vert_71/)), RNA22 (<https://omictools.com/rna22-tool>) and miRDB (<http://www.mirdb.org/>). Moreover, the data analysis website 'TCGA' (<http://www.kmplot.com>), including 1,926 NSCLC patients cases, was used for survival analysis with respect to SGLT2 expression. The negative correlation of miR-296-5p and SGLT2 was determined by Pearson's correlation coefficient.

Differences were considered statistically significant at a value of  $P < 0.05$ .

## Results

**miR-296-5p is downregulated in NSCLC tissues and cells.** The investigation of 46 lung cancer patient datasets (Table I) revealed that miR-296-5p expression was downregulated compared with the corresponding non-tumor lung tissues (Fig. 1A). The analysis of several other datasets (we obtained the corresponding results by analyzing the specific information of the patient tissue samples, such as sex, stage and size), including miRNA expression revealed that the downregulation of miR-296-5p was associated with tumor size (Fig. 1D), but was not associated with pathological stage (Fig. 1B) or sex (Fig. 1C). Moreover, we probed for the expression of miR-296-5p in NSCLC cell lines and found that miR-296-5p was significantly downregulated in the A549, H1299 ( $P < 0.001$ ) and PC-9 cells ( $P < 0.01$ ), compared with the BEAS-2B control normal lung cells (Fig. 1E). These findings indicate that the downregulation of miR-296-5p is associated with NSCLC carcinogenesis.

**miR-296-5p inhibits cell proliferation and cell cycle progression.** To determine whether miR-296-5p affects NSCLC cell proliferation, we first transfected the A549 and H1299 cells with the miR-296-5p mimic. The results of RT-qPCR analysis indicated that miR-296-5p levels were significantly increased in the cells transfected with the miR-296-5p mimic (Fig. 2A). Furthermore, we observed that cellular proliferation gradually decreased with miR-296-5p overexpression in the A549 and H1299 cells. The upregulation of miR-296-5p led to a significant decrease in NSCLC cell growth during a 24-72 h period, when compared with that of the negative control (NC), as assessed by CCK-8 assay (Fig. 2B). Furthermore, the overexpression of miR-296-5p significantly decreased colony-forming ability of the NSCLC cells, as determined by cell colony assays (Fig. 2C). Additionally, G1 arrest was mediated by the upregulation of miR-296-5p after 48 h (Fig. 2D). Overall, our findings demonstrated that miR-296-5p exerts a potential inhibitory effect on tumor formation.

Table III. The sequence of the primers used in this study.

Primer	Sequence
U6 snRNA (F)	5'-CTCGCTTCGGCAGCACA-3'
U6 snRNA (R)	5'-AACGCTTCACGAATTTGCGT-3'
18S RNA (F)	5'-AGGAATTCCAGTAAGTGCG-3'
18S RNA (R)	5'-GCCTCACTAAACCATCCAA-3'
miR-296-5p (qPCR)	5'-AGGGCCCCCCTCAATCCUGT-3
SGLT2 qPCR (F)	5'-GATTACACGGTGACAGGAGGG-3'
SGLT2 qPCR (R)	5'-CGGAGCAGGTGGTAGGAGT-3"
SGLT2-3'-UTR (F)	5'-AGATCGCCGTGTAATTCTAGAGTCAACCTCAATGCCCTGCT-3'
SGLT2-3'-UTR (R)	5'-TCCGGCTGCAGTGCCGAATTCAGGGGAAAGGCAGCTTTATTT-3'
SGLT2-mut3'-UTR (F)	5'-TGCCTCGCGCGACTGCATCTGATTGGCAGTCA-3'
SGLT2-mut3'-UTR (R)	5'-CAGTCGCCGCGAGGCAGAGGAAGGCCGGGAGAA-3'



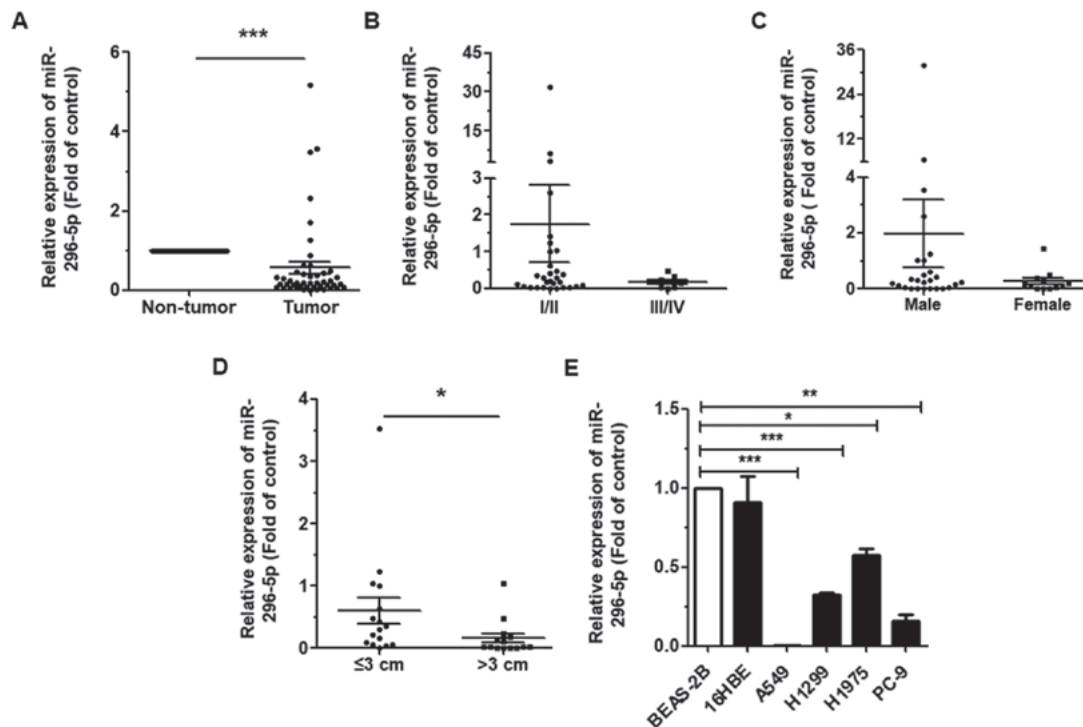


Figure 1. miR-296-5p is downregulated in non-small cell lung cancer (NSCLC) tissues and cells. (A) RT-qPCR analysis of miR-296-5p in non-tumor tissues and corresponding tumor tissues. (B-D) Expression of miR-296-5p was related to tumor pathological stage, sex and size. (E) The expression of miR-296-5p was determined by one-way ANOVA in the 6 human NSCLC cells, followed by Tukey's HSD post-hoc test. BEAS-2B cells were used as the normal control comparison. \*P<0.05, \*\*P<0.01 and \*\*\*P<0.001 compared to the respective control.

*miR-296-5p directly targets SGLT2.* Having identified miR-296-5p as a regulator in NSCLC tissues, we aimed to identify the miR-296-5p targets that mediate the observed effects. We first identified predicted targets of miR-296-5p using 3 different publicly available miRNA target prediction databases (TargetScan, RNA22 and miRDB). Three genes, namely bromo adjacent homology domain containing 1 (*BAHD1*), signal transducer and activator of transcription 3 (*STAT3*) and *SGLT2* were among the predicted miR-296-5p targets present in the 3 databases. *SGLT2* was selected for further analysis (Fig. 3A). To further verify that *SGLT2* is targeted by miR-296-5p, we cloned the 3'-UTR of *SGLT2* into the pGL3 vector, downstream of the luciferase open reading frame (ORF). In addition, to destroy the miR-296-5p binding site, we conducted site-directed mutagenesis of the 3'-UTR using the QuikChange Mutagenesis kit (Fig. 3B). Co-transfection of the 3'-UTR vectors with the miR-296-5p mimic led to a decrease in luciferase activity compared to the miR-control transfection of both the A549 and H1299 cells. By contrast, co-transfection of miR-296-5p mimic with the mutated form of the 3'-UTR resulted in no significant change in luciferase activity (Fig. 3C). Finally, we confirmed the silencing of *SGLT2* by the miR-296-5p mimic at the mRNA and protein levels. The mRNA levels of *SGLT2* decreased in the A549 cells following transfection with the miR-296-5p mimic (Fig. 3D). Of note, the levels of *SGLT2* increased in the H1299 cells, mainly owing to miRNAs being involved in the regulation of the post-transcriptional of gene expression. The mechanisms of action are complex. miRNAs function mainly in two ways, one is the degradation of mRNA, and the other is to inhibit translation, playing a role in protein levels. Western blot analysis clearly indicated that the inhibitory effects of miR-296-5p are

mediated, at least in part, by the targeting of *SGLT2*, as the protein expression of *SGLT2* markedly decreased in the cells transfected with the miR-296-5p mimic (Fig. 3E and F). On the whole, these data suggest that miRNA can specifically target the 3'-UTR of *SGLT2* in the A549 and H1299 cells.

*SGLT2 is upregulated in NSCLC tissues and cells.* To determine whether the expression of *SGLT2* is affected by miR-296-5p, the expression of *SGLT2* was detected in 46 tissues (Table I). Among the pairs of tissues, *SGLT2* expression was upregulated relative to the matched para-cancerous tissues (P<0.05; Fig. 4A), but was not associated with pathological stage (Fig. 4B), sex (Fig. 4C), or tumor size (Fig. 4D). Therefore, based on the Pearson's correlation coefficient, miR-296-5p was found to negatively correlate with *SGLT2* (Fig. 4E).

Finally, we examined the effects of *SGLT2* expression in lung cancer patients. We used the Kaplan-Meier Plotter online database ([www.kmplot.com/analysis](http://www.kmplot.com/analysis)) (Fig. 4F) to generate a Kaplan-Meier survival curve of the patients with NSCLC with a low or high expression of *SGLT2*. Among the 1,926 cases, patients with NSCLC with a high expression of *SGLT2* had lower survival rates.

*Effects of the inhibition of SGLT2 on cell proliferation and cell cycle progression.* To determine whether the biological effects of miR-296-5p may be attributed to the direct targeting of *SGLT2*, we silenced its expression using siRNA and detected alterations in cell proliferation and cell cycle progression, as previously described (26,34). Transfection of the NSCLC cells with *SGLT2*-directed siRNA suppressed the *SGLT2* mRNA (Fig. 5A) and protein (Fig. 5B and C) levels, as compared to the

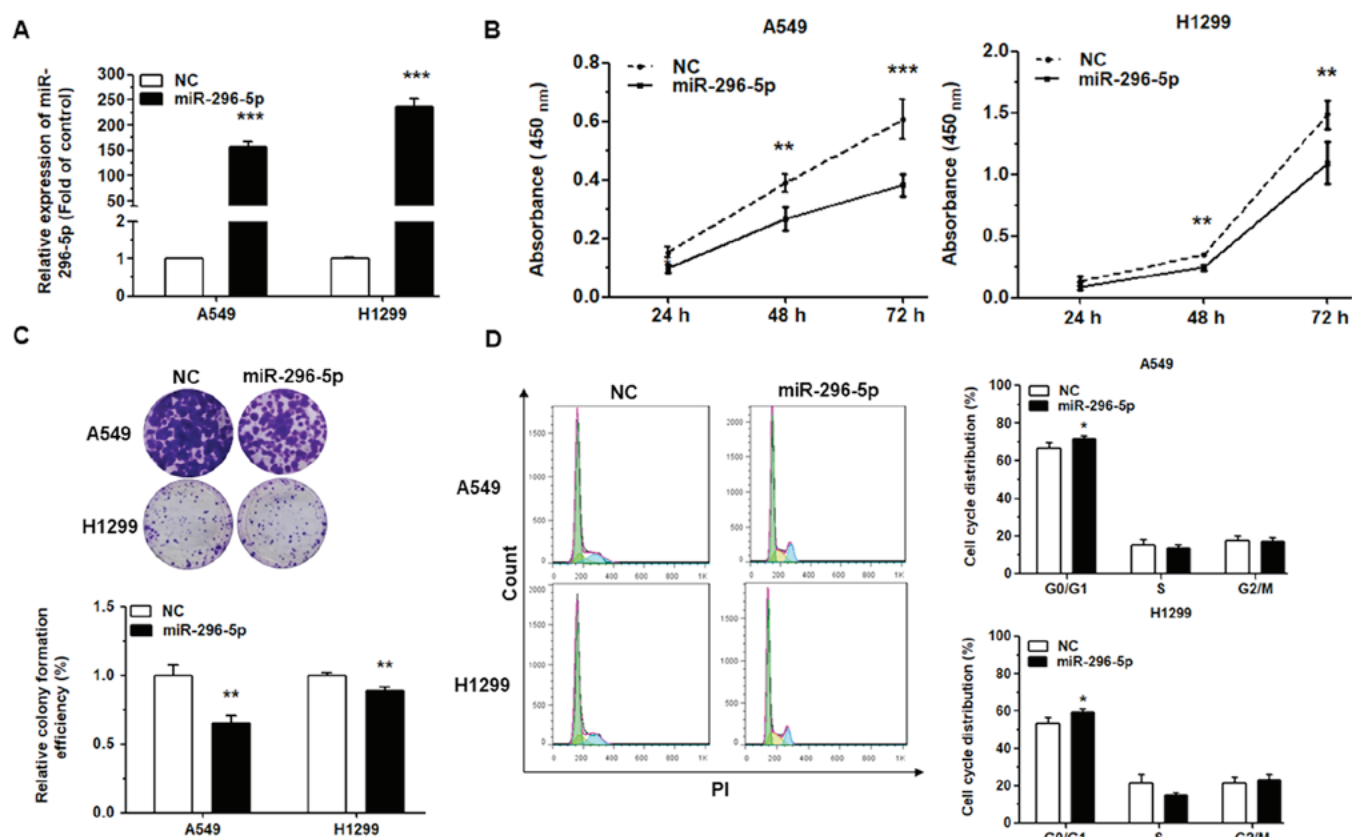


Figure 2. miR-296-5p can inhibit cell proliferation and cell cycle progression. (A) Transfected A549 and H1299 cells analyzed by RT-qPCR. (B) The proliferation of A549 and H1299 cell lines, as measured by Cell Counting Kit-8 (CCK-8) assay, following transfection with the miR-296-5p mimic. (C) Colony formation assay in A549 and H1299 cells. (D) The cell cycle distribution of A549 and H1299 cells transfected with negative control (NC) or the miR-296-5p mimic detected by flow cytometry. \* $P < 0.05$ , \*\* $P < 0.01$  and \*\*\* $P < 0.001$  compared to the control.

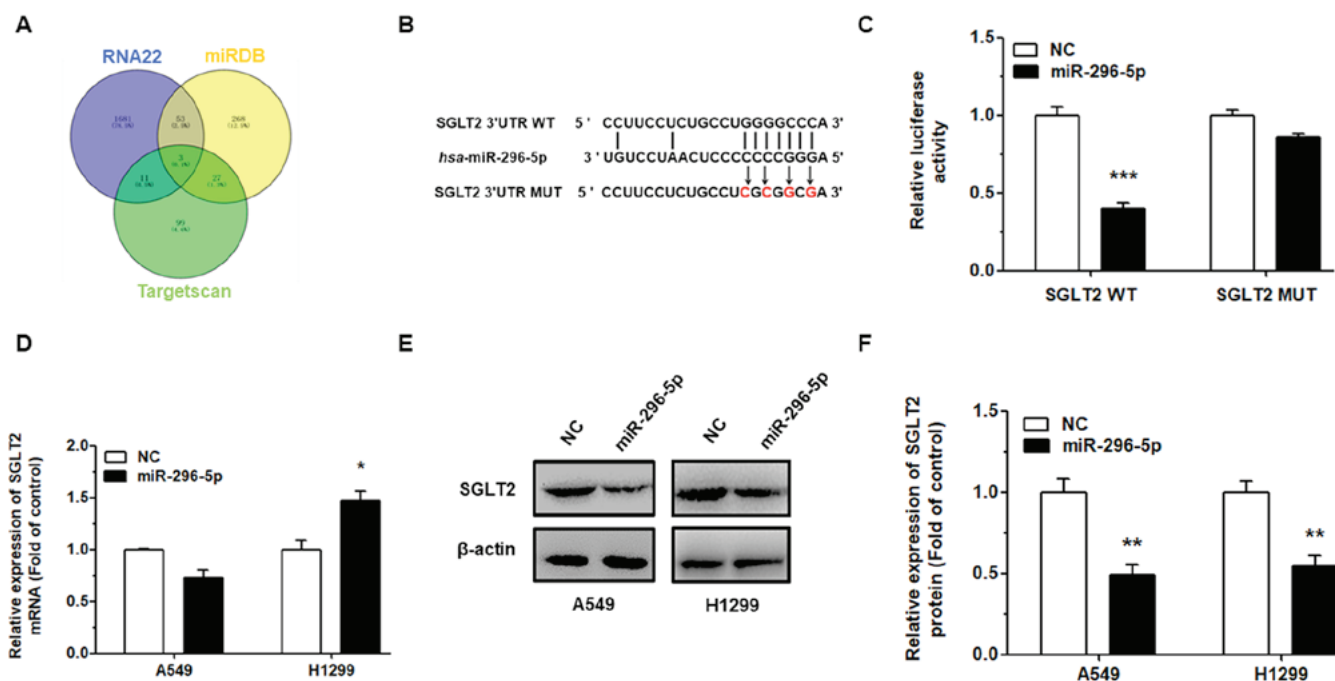


Figure 3. miR-296-5p directly targets sodium-glucose co-transporter-2 (*SGLT2*). (A) Bioinformatics identification of miR-296-5p target candidates. Blue circle, the predicted targets generated by RNA22; yellow circle, the predicted targets generated by miRDB; green circle, the predicted targets generated by TargetScan. (B) *SGLT2* is significantly regulated by the expression of miR-296-5p. (C) 293T cells expressing wild-type (WT) and mutant (MUT) *SGLT2* 3'-UTR mutant reporter constructs co-transfected with the miR-296-5p mimic and analyzed for luciferase activity. (D and E) A549 and H1299 cells transfected with the miR-296-5p mimic and then examined for *SGLT2* expression after 48 h. *SGLT2* mRNA and protein levels were analyzed by RT-qPCR and western blot analyses, respectively. (F) Densitometry was used to quantify the relative expression of *SGLT2* proteins, following normalization to  $\beta$ -actin. \* $P < 0.05$ , \*\* $P < 0.01$  and \*\*\* $P < 0.001$  compared to the control.

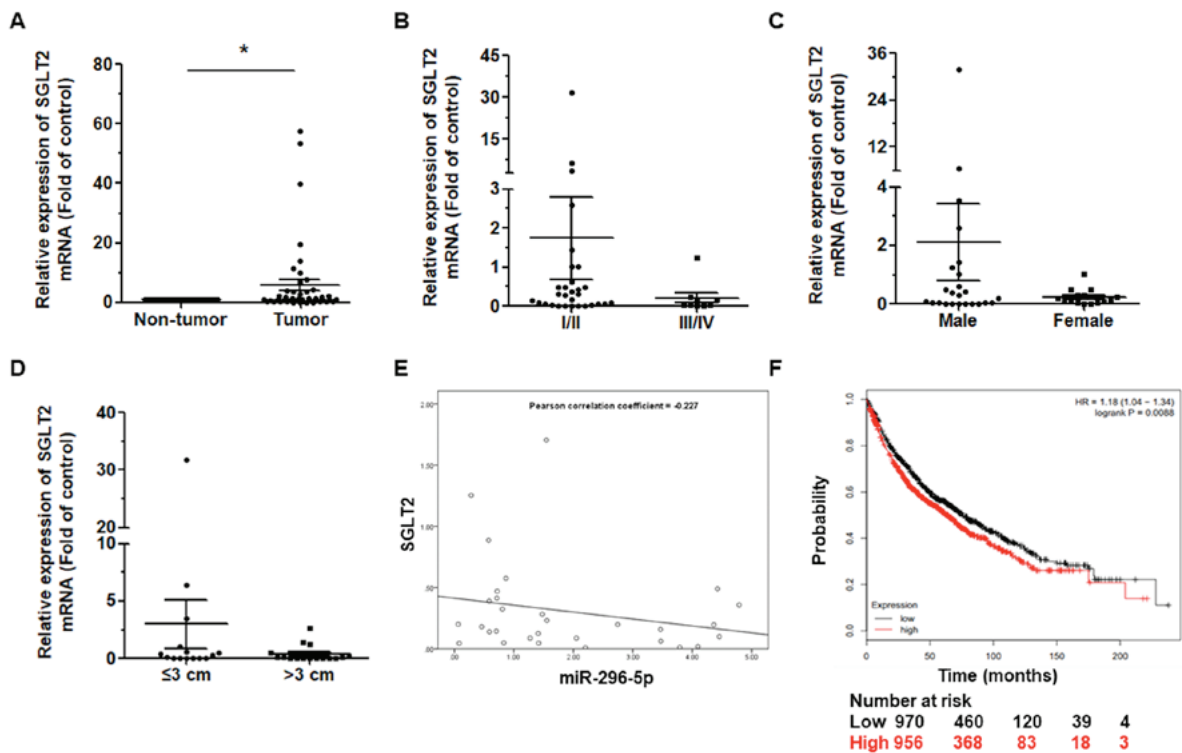


Figure 4. Sodium-glucose co-transporter-2 (*SGLT2*) is upregulated in tumor tissues and cancer cells. (A) Comparative expression of *SGLT2* in 46 patients with lung cancer by RT-qPCR. (B-D) Expression of *SGLT2* was related to tumor pathological stage, sex and size. (E) Negative correlation between miR-296-5p and *SGLT2*, according to the Pearson's correlation coefficient. (F) The effect of *SGLT2* expression levels on the overall survival of 1,926 lung cancer patients. Kaplan-Meier plots were generated using a Kaplan-Meier Plotter. \*P<0.05, compared to the control.

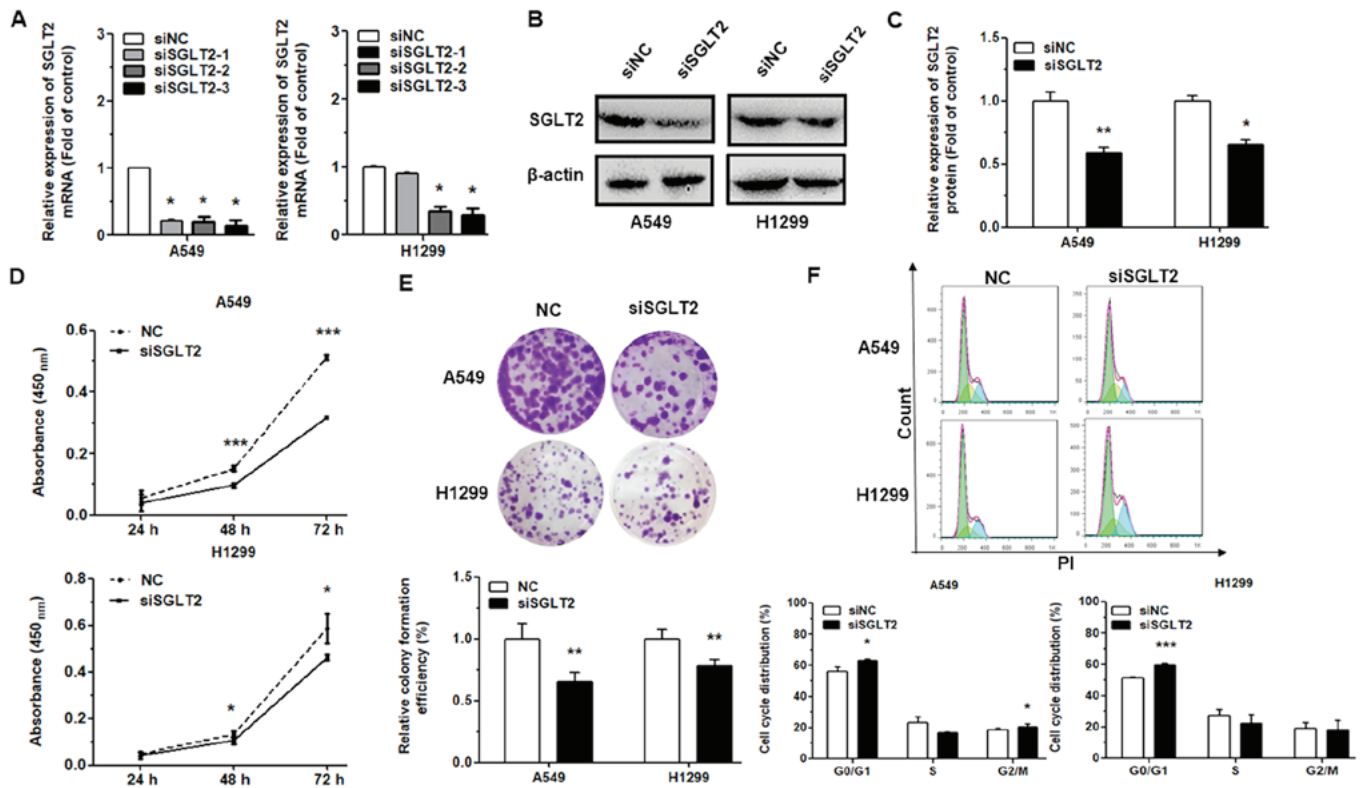


Figure 5. Effect of sodium-glucose co-transporter-2 (*SGLT2*) inhibition on proliferation and cell cycle. (A and B) A549 and H1299 cells transfected with control non-targeting or *SGLT2*-directed siRNA and analyzed by RT-qPCR and western blot analysis, respectively. (C) Densitometric quantification of the relative expression of *SGLT2* protein, following normalization to β-actin, in A549 and H1299 cells transfected with siRNA against *SGLT2* (siSGLT2). (D) A549 and H1299 cells transfected with siSGLT2 and analyzed by CCK-8 assay. (E) A549 and H1299 cells transfected with siSGLT2 used in colony formation assays. (F) The cell cycle distributions of A549 and H1299 cells transfected with siSGLT2 as detected by flow cytometry. \*P<0.05, \*\*P<0.01 and \*\*\*P<0.001 compared to the control.

control. Moreover, the results of CCK-8 and cell colony assays revealed that the proliferative capacity of the NSCLC cells was significantly downregulated at 72 h following transfection with siSGLT2 (Fig. 5D and E). We also found that at 48 h following *SGLT2* knockdown, the proportion of cells in the G0/G1 phase increased as compared with the control (Fig. 5F). Taken together, our data highlight that the observed effects of miR-296-5p on cell proliferation and cell cycle progression are mediated by the targeting of *SGLT2*.

## Discussion

Lung cancer does not have an exact cause, as some environmental factors, such as tobacco, radon, asbestos and other industrial carcinogens may increase the risk of developing lung cancer (8,35,36). NSCLC has a high incidence and high mortality, and has become the focus of research in recent years (37). However, the specific mechanisms of NSCLC remain unclear, and further investigations are required into this matter. The dysregulation of miRNAs has been linked to the development of various types of human cancer. Recently, increasing evidence supports the notion that the aberrant expression of miRNAs plays critical roles in NSCLC occurrence and progression (38,39) miRNAs can function as oncogenes or tumor suppressors (40,41). Our previous studies confirmed that miRNAs, such as miR-34a (32), miR-486-5p (42) and miR-181a-5p(43) can function as tumor suppressor genes, while miR-18a-5p (28) and miR-150 (44) can function as oncogenes in NSCLC.

Previous findings have established miR-296-5p as a tumor suppressor through its ability to suppress cancer cells in different types of cancer (45-48). However, the roles of miR-296-5p in lung cancer tumorigenesis and the underlying mechanisms have not yet been completely reported. Therefore, in this study, we investigated the potential functions of miR-296-5p in the development and progression of NSCLC. Our results revealed that miR-296-5p was downregulated in the majority of the NSCLC patient samples examined and in several NSCLC cell lines. Moreover, we found that the low expression of miR-296-5p was related to tumor size according to case information analysis after measuring the expression of miR-296-5p in 46 pairs of patients by RT-qPCR. When the tumor is small, the expression of miR-296-5p is relatively high and in larger tumors, the expression of miR-296-5p relatively low, which is consistent with the role of miR-296-5p as a tumor suppressor in lung cancer. In addition, our data confirmed miR-296-5p as a tumor suppressor in lung cancer and that it directly targets *SGLT2*. In the future, we aim to further investigate the roles of miR-296-5p in suppressing invasiveness and the cell migratory capability *in vitro* and *in vivo*.

The findings of this study, and other studies shed some light into the role of miR-296-5p in regulating cancer. It has also been found that miR-296-5p plays an important role in diabetes mellitus (DM), which is regulated by *SGLT2* (24,49-52). This study confirmed that miR-296-5p can suppress DM by targeting *SGLT2* (data not shown). Therefore, miR-296 may have more functions than previously anticipated.

In conclusion, the present study demonstrates that miR-296-5p functions as a tumor suppressor in NSCLC by targeting *SGLT2*. Our findings provide a further understanding

of the potential mechanisms through which miRNAs affect the development and oncogenesis of NSCLC. The findings of this study may aid in the development of more effective treatment strategies for NSCLC. Moreover, miR-296-5p may prove to be a useful prognostic marker for NSCLC.

## Acknowledgements

The authors acknowledge Miss Fatemeh Alsadat Jafari Sheshtamad (Mashhad University of Medical Science, Mashhad, Iran) for the critical reading of the manuscript. The authors would also like to thank her for her valuable comments and suggestions and for the language editing of the article.

## Funding

This study was funded by the National Natural Science Foundation (grant no. 81601887).

## Availability of data and materials

The datasets used and/or analyzed during the current study are available from the corresponding author on reasonable request.

## Authors' contributions

XIAOTIAN Z and XINJU Z conceived the experiments; XL developed the methodology; PQ and HW analyzed and interpreted the data; ZM and YC were involved in the conception and design of the study and edited the manuscript. All authors have read and approved the final manuscript.

## Ethics approval and consent to participate

The use of patient samples was approved by the Ethics Committee of Shanghai Hospital and consent was obtained from all the patients.

## Patient consent for publication

Not applicable.

## Competing interests

The authors declare that they have no competing interests.

## References

1. Torre LA, Bray F, Siegel RL, Ferlay J, Lortet-Tieulent J and Jemal A: Global cancer statistics, 2012. *CA Cancer J Clin* 65: 87-108, 2015.
2. Chen W, Zheng R, Baade PD, Zhang S, Zeng H, Bray F, Jemal A, Yu XQ and He J: Cancer statistics in China, 2015. *CA Cancer J Clin* 66: 115-132, 2016.
3. Xu C, Li S, Chen T, Hu H, Ding C, Xu Z, Chen J, Liu Z, Lei Z, Zhang HT, *et al*: miR-296-5p suppresses cell viability by directly targeting PLK1 in non-small cell lung cancer. *Oncol Rep* 35: 497-503, 2016.
4. Lozano R, Naghavi M, Foreman K, Lim S, Shibuya K, Aboyans V, Abraham J, Adair T, Aggarwal R, Ahn SY, *et al*: Global and regional mortality from 235 causes of death for 20 age groups in 1990 and 2010: A systematic analysis for the Global Burden of Disease Study 2010. *Lancet* 380: 2095-2128, 2012.



5. Jain RK and Chen H: Spotlight on brigatinib and its potential in the treatment of patients with metastatic ALK-positive non-small cell lung cancer who are resistant or intolerant to crizotinib. *Lung Cancer (Auckl)* 8: 169-177, 2017.
6. Goffin J, Lacchetti C, Ellis PM, Ung YC and Evans WK: Lung Cancer Disease Site Group of Cancer Care Ontario's Program in Evidence-Based Care: First-line systemic chemotherapy in the treatment of advanced non-small cell lung cancer: A systematic review. *J Thorac Oncol* 5: 260-274, 2010.
7. Gao Y, Gao F, Ma JL, Sun WZ and Song LP: The potential clinical applications and prospects of microRNAs in lung cancer. *OncoTargets Ther* 7: 901-906, 2014.
8. Kanwal M, Ding XJ and Cao Y: Familial risk for lung cancer. *Oncol Lett* 13: 535-542, 2017.
9. Ye Y, Li SL and Wang SY: Construction and analysis of mRNA, miRNA, lncRNA, and TF regulatory networks reveal the key genes associated with prostate cancer. *PLoS One* 13: e0198055, 2018.
10. Morales S, De Mayo T, Gulppi FA, Gonzalez-Hormazabal P, Carrasco V, Reyes JM, Gómez F, Waugh E and Jara L: Genetic variants in pre-miR-146a, pre-miR-499, pre-miR-125a, pre-miR-605, and pri-miR-182 are associated with breast cancer Ssusceptibility in a South American Population. *Genes (Basel)* 9: 9, 2018.
11. Tian W, Du Y, Ma Y, Gu L, Zhou J and Deng D: MALAT1-miR663a negative feedback loop in colon cancer cell functions through direct miRNA-lncRNA binding. *Cell Death Dis* 9: 857, 2018.
12. Dua K, Hansbro NG, Foster PS and Hansbro PM: MicroRNAs as therapeutics for future drug delivery systems in treatment of lung diseases. *Drug Deliv Transl Res* 7: 168-178, 2017.
13. Cho WC: MicroRNAs: Potential biomarkers for cancer diagnosis, prognosis and targets for therapy. *Int J Biochem Cell Biol* 42: 1273-1281, 2010.
14. Bartels CL and Tsongalis GJ: MicroRNAs: Novel biomarkers for human cancer. *Clin Chem* 55: 623-631, 2009.
15. Bowen T, Jenkins RH and Fraser DJ: MicroRNAs, transforming growth factor beta-1, and tissue fibrosis. *J Pathol* 229: 274-285, 2013.
16. Fu Q, Song X, Liu Z, Deng X, Luo R, Ge C, Li R, Li Z, Zhao M, Chen Y, *et al*: miRomics and proteomics reveal a miR-296-3p/PRKCA/FAK/Ras/c-Myc feedback loop modulated by HDGF/DDX5/ $\beta$ -catenin complex in lung adenocarcinoma. *Clin Cancer Res* 23: 6336-6350, 2017.
17. Vaira V, Favarsani A, Dohi T, Montorsi M, Augello C, Gatti S, Coggi G, Altieri DC and Bosari S: miR-296 regulation of a cell polarity-cell plasticity module controls tumor progression. *Oncogene* 31: 27-38, 2012.
18. Savi F, Forno I, Favarsani A, Luciani A, Caldiera S, Gatti S, Foa P, Ricca D, Bulfamante G, Vaira V, *et al*: miR-296/Scribble axis is deregulated in human breast cancer and miR-296 restoration reduces tumour growth in vivo. *Clin Sci (Lond)* 127: 233-242, 2014.
19. Barbagallo D, Piro S, Condorelli AG, Mascali LG, UrbanoF, Parrinello N, Monello A, Statello L, Ragusa M, Rabuazzo AM, *et al*: miR-296-3p, miR-298-5p and their downstream networks are causally involved in the higher resistance of mammalian pancreatic  $\alpha$  cells to cytokine-induced apoptosis as compared to  $\beta$  cells. *BMC Genomics* 14: 62, 2013.
20. Carreras-Badosa G, Bonmatí A, Ortega FJ, Mercader JM, Guindo-Martínez M, Torrents D, Prats-Puig A, Martínez-Calcerrada JM, de Zegher F, Ibáñez L, *et al*: Dysregulation of placental miRNA in maternal obesity is associated with pre- and postnatal growth. *J Clin Endocrinol Metab* 102: 2584-2594, 2017.
21. Togliatto G, Dentelli P, Rosso A, Lombardo G, Gili M, Gallo S, Gai C, Solini A, Camussi G and Brizzi MF: PDGF-BB carried by endothelial cell-derived extracellular vesicles reduces vascular smooth muscle cell apoptosis in diabetes. *Diabetes* 67: 704-716, 2018.
22. Shivapurkar N, Mikhail S, Navarro R, Bai W, Marshall J, Hwang J, Pishvaian M, Wellstein A and He AR: Decrease in blood miR-296 predicts chemotherapy resistance and poor clinical outcome in patients receiving systemic chemotherapy for metastatic colon cancer. *Int J Colorectal Dis* 28: 887, 2013.
23. Wang L, Bo X, Zheng Q, Xiao X, Wu L and Li B: miR-296 inhibits proliferation and induces apoptosis by targeting FGFR1 in human hepatocellular carcinoma. *FEBS Lett* 590: 4252-4262, 2016.
24. Gallo LA, Wright EM and Vallon V: Probing SGLT2 as a therapeutic target for diabetes: Basic physiology and consequences. *Diab Vasc Dis Res* 12: 78-89, 2015.
25. Scafoglio C, Hirayama BA, Kepe V, Liu J, Ghezzi C, Satyamoorthy N, Moatamed NA, Huang J, Koepsell H, Barrio JR, *et al*: Functional expression of sodium-glucose transporters in cancer. *Proc Natl Acad Sci USA* 112: E4111-E4119, 2015.
26. Ishikawa N, Oguri T, Isobe T, Fujitaka K and Kohno N: SGLT gene expression in primary lung cancers and their metastatic lesions. *Jpn J Cancer Res* 92: 874-879, 2001.
27. Yao Y, Shao J, Wu J, Zhang Q, Wang J, Xiao D and Huang F: The functional variant in the 3'UTR of PTPRT with the risk of esophageal squamous cell carcinoma in a Chinese population. *Cell Physiol Biochem* 36: 306-314, 2015.
28. Liang C, Zhang X, Wang HM, Liu XM, Zhang XJ, Zheng B, Qian GR and Ma ZL: MicroRNA-18a-5p functions as an oncogene by directly targeting IRF2 in lung cancer. *Cell Death Dis* 8: e2764, 2017.
29. Livak KJ and Schmittgen TD: Analysis of relative gene expression data using real-time quantitative PCR and the 2(-Delta Delta C(T)) Method. *Methods* 25: 402-408, 2001.
30. Shao Y, Sun Q, Liu X, Wang P, Wu R and Ma Z: tRF-Leu-CAG promotes cell proliferation and cell cycle in non-small cell lung cancer. *Chem Biol Drug Des* 90: 730-738, 2017.
31. Zhang B, Ma Z, Li X, Zhang C, Shao Y, Liu Z, Li Y and Jin Y: Tanshinones suppress non-small cell lung cancer through up-regulating miR-137. *Acta Biochim Biophys Sin (Shanghai)* 48: 768-770, 2016.
32. Li YL, Liu XM, Zhang CY, Zhou JB, Shao Y, Liang C, Wang HM, Hua ZY, Lu SD and Ma ZL: MicroRNA-34a/EGFR axis plays pivotal roles in lung tumorigenesis. *Oncogenesis* 6: e372, 2017.
33. Wang P, Liu X, Shao Y, Wang H, Liang C, Han B and Ma Z: MicroRNA-107-5p suppresses non-small cell lung cancer by directly targeting oncogene epidermal growth factor receptor. *Oncotarget* 8: 57012-57023, 2017.
34. Hine J, Paterson H, Abrol E, Russell-Jones D and Herring R: SGLT inhibition and euglycaemic diabetic ketoacidosis. *Lancet Diabetes Endocrinol* 3: 503-504, 2015.
35. Brinker TJ, Alftian J, Seeger W, Groneberg DA, von Kalle C, Enk AH, Herth FJF, Kreuter M, Bauer CM, Gatzka M, *et al*: A face-aging smoking prevention/cessation intervention for nursery school students in Germany: An appearance-focused interventional study. *Int J Environ Res Public Health* 15: 15, 2018.
36. Ma H, Chen X, Hu H, Li B, Ying X, Zhou C, Zhong J, Zhao G and Duan S: Hypermethylation of MDFI promoter with NSCLC is specific for females, non-smokers and people younger than 65. *Oncol Lett* 15: 9017-9024, 2018.
37. Cheong HT, Xu F, Choy CT, Hui CWC, Mok TSK and Wong CH: Upregulation of Bcl2 in NSCLC with acquired resistance to EGFR-TKI. *Oncol Lett* 15: 901-907, 2018.
38. Romero-Cordoba SL, Salido-Guadarrama I, Rodriguez-Dorantes M and Hidalgo-Miranda A: miRNA biogenesis: Biological impact in the development of cancer. *Cancer Biol Ther* 15: 1444-1455, 2014.
39. Tutar Y: miRNA and cancer; computational and experimental approaches. *Curr Pharm Biotechnol* 15: 429, 2014.
40. Ji W, Sun B and Su C: Targeting microRNAs in cancer gene therapy. *Genes (Basel)* 8: 8, 2017.
41. Ebrahimi A and Sadroddiny E: MicroRNAs in lung diseases: Recent findings and their pathophysiological implications. *Pulm Pharmacol Ther* 34: 55-63, 2015.
42. Shao Y, Shen YQ, Li YL, Liang C, Zhang BJ, Lu SD, He YY, Wang P, Sun QL, Jin YX, *et al*: Direct repression of the oncogene CDK4 by the tumor suppressor miR-486-5p in non-small cell lung cancer. *Oncotarget* 7: 34011-34021, 2016.
43. Ma Z, Qiu X, Wang D, Li Y, Zhang B, Yuan T, Wei J, Zhao B, Zhao X, Lou J, *et al*: miR-181a-5p inhibits cell proliferation and migration by targeting Kras in non-small cell lung cancer A549 cells. *Acta Biochim Biophys Sin (Shanghai)* 47: 630-638, 2015.
44. Wang DT, Ma ZL, Li YL, Wang YQ, Zhao BT, Wei JL, Qi X, Zhao XT and Jin YX: miR-150, p53 protein and relevant miRNAs consist of a regulatory network in NSCLC tumorigenesis. *Oncol Rep* 30: 492-498, 2013.
45. Lee H, Shin CH, Kim HR, Choi KH and Kim HH: MicroRNA-296-5p promotes invasiveness through downregulation of nerve growth factor receptor and caspase-8. *Mol Cells* 40: 254-261, 2017.
46. Lee KH, Lin FC, Hsu TI, Lin JT, Guo JH, Tsai CH, Lee YC, Lee YC, Chen CL, Hsiao M, *et al*: MicroRNA-296-5p (miR-296-5p) functions as a tumor suppressor in prostate cancer by directly targeting Pin1. *Biochim Biophys Acta* 1843: 2055-2066, 2014.

47. Li T, Lu YY, Zhao XD, Guo HQ, Liu CH, Li H, Zhou L, Han YN, Wu KC, Nie YZ, *et al*: MicroRNA-296-5p increases proliferation in gastric cancer through repression of Caudal-related homeobox 1. *Oncogene* 33: 783-793, 2014.
48. Maia D, de Carvalho AC, Horst MA, Carvalho AL, Scapulatempo-Neto C and Vettore AL: Expression of miR-296-5p as predictive marker for radiotherapy resistance in early-stage laryngeal carcinoma. *J Transl Med* 13: 262, 2015.
49. Watanabe A, Choe S, Chaptal V, Rosenberg JM, Wright EM, Grabe M and Abramson J: The mechanism of sodium and substrate release from the binding pocket of vSGLT. *Nature* 468: 988-991, 2010.
50. Cramer SC, Pardridge WM, Hirayama BA and Wright EM: Colocalization of GLUT2 glucose transporter, sodium/glucose cotransporter, and gamma-glutamyl transpeptidase in rat kidney with double-peroxidase immunocytochemistry. *Diabetes* 41: 766-770, 1992.
51. Vallon V, Rose M, Gerasimova M, Satriano J, Platt KA, Koepsell H, Cunard R, Sharma K, Thomson SC and Rieg T: Knockout of Na-glucose transporter SGLT2 attenuates hyperglycemia and glomerular hyperfiltration but not kidney growth or injury in diabetes mellitus. *Am J Physiol Renal Physiol* 304: F156-F167, 2013.
52. Chao EC and Henry RR: SGLT2 inhibition--a novel strategy for diabetes treatment. *Nat Rev Drug Discov* 9: 551-559, 2010.